2011 IEEE/RSJ International Conference on
Intelligent Robots and Systems
September 25-30, 2011. San Francisco, CA, USA

The sigma.7 haptic interface for MiroSurge: A new bi-manual surgical console

Andreas Tobergte, Patrick Helmer, Ulrich Hagn, Patrice Rouiller, Sophie Thielmann, Sébastien Grange, Alin Albu-Schäffer, François Conti, and Gerd Hirzinger

Abstract— **This paper presents the design and control of the sigma.7 haptic device and the new surgical console of the MiroSurge robotic system. The console and the haptic devices are designed with respect to requirements in minimally invasive robotic surgery. Dedicated left and right handed devices are integrated in an operator console in an ergonomic configuration. The height of the whole console is adjustable, allowing the surgeon seated and standed operation. Each of the devices is fully actuated in seven degrees of freedom (DoF). A parallel mechanism with 3 DoF actuates the translational motion and an attached wrist with 3 intersecting axis drives the rotations of the grasping unit. This advantageous design leads to inherently decoupled kinematics and dynamics. Cartesian forces are 20 N within the translational workspace, which is a sphere of about 120 mm diameter for each device. The rotational wrist of the device covers the whole workspace of the human hand and provides maximum torques of about 0.4 Nm. The grasping unit can display forces up to 8 N. An integrated force/torque sensor is used to increase the transparency of the devices by reducing inertia and friction. It is theoretically shown that the non-linear closed loop system behaves like a passive system and experimental results validate the approach. The sigma.7 haptic devices are designed by Force Dimension in cooperation with the German Aerospace Center (DLR). DLR designed the surgical console and integrated the haptic devices in the MiroSurge system.**

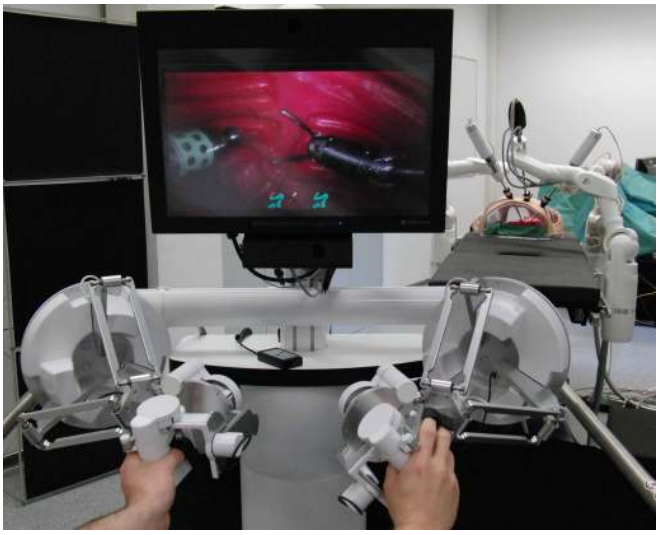

Fig. 1. Foreground: Operator console with bi-manual sigma.7 and auto-stereoscopic display; Background: Three MIRO arms attached to an operating table, two holding MICA instruments and one holding a stereo endoscope

I. INTRODUCTION

Minimally invasive robotic surgery (MIRS) is an emerging technology to overcome the drawbacks of minimally invasive surgery. Among these drawbacks are the loss of hand-eye coordination due to motion inversion with the invariant fulcrum point and an unergonomic working pose for the surgeon. Motion is restricted inside the patient, due to the entry point that binds two DoF. The haptic perception is disturbed by the friction at the entry point and the long flexible instruments. Robotic surgery is an approach to overcome these drawbacks. The surgeon can operate the robotic instruments inside the patient in an intuitive manner from an operator station, as shown in Fig. 1. The MiroSurge system from DLR (German Aerospace Center) is a prototype for minimally invasive robotic surgery [7] [8]. It is based on the versatile light weight robot MIRO [18], that serves as an instrument carrier. The MICA instruments [15] are actuated in in three DoF, a dedicated wrist joint offers two DoF to regain 6 DoF manipulability inside the patient. A third motor actuates a functional tip of the instrument, e.g. surgical forceps. A unique feature of the MICA instrument is the force/torque sensing capability for manipulation of tissue. A seven DoF force/torque sensor in the tip can measure manipulation forces/torques and the grasping force [13]. In bi-lateral teleoperation the interaction forces can be fed back to haptic devices controlled by the human operator [16] [17], allowing for sensitive manipulation and palpation.

A key component in bilateral teleoperation is the haptic device. Available haptic devices can be separated into 3 classes: 1) Compact table top devices, in general have low inertia and a workspace designed for user interaction with the hand and the forearm. Typical devices including torque feedback are the PHANTOM Premium (SensAble Technologies, Inc., USA) [1], the Virtuose 6D Desktop (Haption, S.A., France), the DELTA.6 Haptic Device from Force Dimension [6] and the Freedom-7 [2]. 2) Larger robotic arms, such as the Virtuose 6D35-45 from Haption or the DLR/KUKA Light-Weight Robot (LWR) [9] offer a huge workspace, so that the user can work with his whole arm but have inevitable higher inertia or lower stiffness than table top devices. 3) The third

Andreas Tobergte, Ulrich Hagn, Sophie Thielmann, Alin Albu-Schäffer, and Gerd Hirzinger are with Institute of Robotics and Mechatronics, DLR - German Aerospace Center, Wessling, Germany andreas.tobergte, ulrich.hagn, sophie.thielmann, alin.albu-schaeffer, gerd.hirzinger@dlr.de

Patrick Helmer, Patrice Rouiller, Sébastien Grange and François Conti are with Force Dimension, Nyon, Switzerland helmer, rouiller, grange, conti@forcedimension.com

category are exoskeletons, that also allow haptic interaction in the null-space, e.g. the elbow.

The haptic devices for the MiroSurge operator console, should basically match the category of a table top device with low inertia and low friction for fine manipulation and palpation. It should be fully actuated in 6 Cartesian DoF and provide a grasping unit for interacting with the gripper of the MICA instrument. The translational workspace should coarsely match the one of the human forearm, when it is resting on a pad. The rotational motion range is to be large enough for unrestricted suturing gestures. Continuous force output has to be at least $10N$ to match the specifications of the sensor in the MICA instrument. Ideally, the device should be statically and dynamically balanced around the center of rotation in the human hand to minimize the effects of the mechanical coupling on the user's perception. Inertia and friction should be low and the structure of the device should be stiff. Because requirements on motor actuation and stiffness will inevitably lead to a considerable mass, integrated force/torque sensing is required for closed loop reduction of inertia. A high degree of transparency should improve the ability to discriminate fine stiffness variations, e.g. for localizing tumors. Finally, two devices are to be integrated in a surgical console, where the human operator can bring his hands as closely together as possible.

Since none of the available haptic devices was found to fully meet the requirements for a new MiroSurge console, DLR started a collaboration with Force Dimension in 2009. After one year of development, the new surgical console was first presented at the Automatica 2010 trade fare in Munich. The custom sigma.7 haptic devices were developed by Force Dimension meeting the DLR specific requirements. The console design, control, and integration in MiroSurge was done by DLR. In 2011 Force Dimension started to offer a modified commercial version of the sigma.7. The most significant difference is that the commercial version does not integrate force/torque sensing.

In the following section II the design of the sigma.7 and the surgical console is described. Details of the device kinematics and dynamics are presented in section III. The control of the DLR customized device is described in section IV with theoretical analysis and experiments. Section V concludes the paper and gives an outlook on future work.

II. Device and console design

In this section the design of the sigma.7 haptic device and the MiroSurge surgical console is described. The design originates from the omega.7, that has passive rotations without motors and does not have force/torque sensing. The omega.7 from Force Dimension, as a typical table top device, was previously used in the MiroSurge system, as shown in Fig. 2.

A. Haptic device

The electromechanical structure of the sigma.7 haptic input device comprises three main components: translational base, rotational wrist extension and grasping unit.

Fig. 2. Foreground: Two omega.7 as master devices; Background: Three Miro robots at an operating table

The translational base has a parallel kinematics structure of the "delta" family [6] with three independent kinematics chains fixed to the device base and jointed together at the translational base output. The first arm of each chain is driven by a torque actuator in form of an electric motor engaging with the chain's first arm through a cable transmission ensuring smooth and stiff force transmission without mechanical play. The motors are custom designed and optimized with respect to friction, torque and torque smoothness at low rotational speeds. Each motor has a high resolution incremental encoder to measure rotational position of its output shaft. The parallel bar arrangement which connects the output of the first arm of each chain and the translational base output stiffly lock any rotational motion of the latter. The workspace has been designed to include a spherical volume of 120 mm in diameter, compatible with the forearm motion of a seated operator. It is virtually limited to this sphere with the motors and can be increased (up to 130mm, 190mm, 190mm in x, y, z) if the full forces, as specified in TABLE I are not needed. Maximum continuous force output is about 20N after gravity is compensated. In the commercial version of the sigma.7 gravity compensation is passively supported by a spring, which is not used in the custom DLR design.

The rotational wrist extension is mounted on the translational base output and has a serial kinematics structure with an arrangement of three pivot joints having intersecting axes in the hand-center-point (HCP). The axis are mutually orthogonal in a nominal posture, as shown in Fig. 4. Actuation and transmission means are similar to the ones used for the translational base. The spatial layout of the rotational wrist parts has been optimized with respect to inertia and total weight, since the latter is entirely carried by the translational base. Angular motion range has been optimized to allow for nearly unrestrained motion of the operator's wrist, compatible with demanding suturing gestures.

The grasping unit is mounted on the wrist extension output and provides 2 members: a fixed member including a hand grip and a movable member with an interface for the index

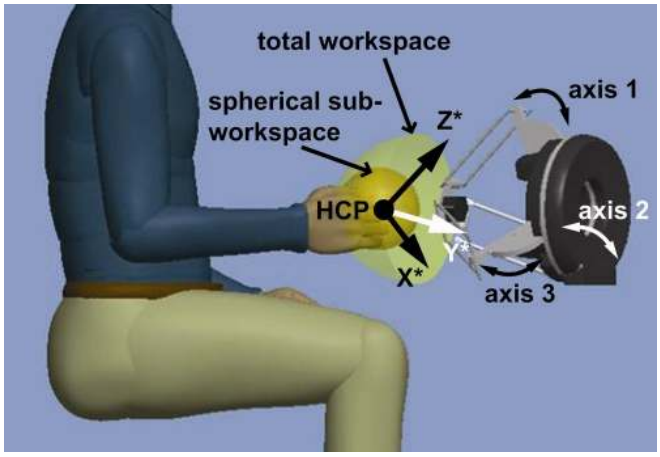

Fig. 3. sigma.7 with spherical workspace; translational base with axes 1,2,3, counter clockwise order, starting from the top; hand-center-point (HCP) as frame of reference

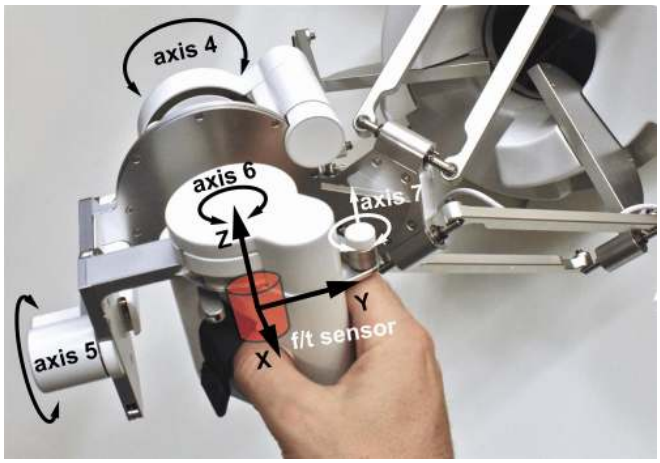

Fig. 4. Perpendicular axes of the rotational wrist with force-/torque sensor in the intersection point (HCP-frame) integrated in the mechanical structure; grasping unit (handle) attached to the sensor

finger and forefinger. Actuation and transmission means are similar to the ones used for the translational base. In fact, the highly integrated hand grip encloses not only the grasping unit actuator, but also the actuator of the third wrist joint as well as a 6 DoF force/torque sensor (model Nano17 from ATI, Inc., USA). This sensor is inserted between rotational wrist output and grasping unit in the HCP. Grooves for the thumb on the hand grip as well as for the index finger on the movable member are equipped with adjustable straps thus enabling bi-directionality of the grasping force. The movable member has a rotation axis parallel to the third joint axis of the wrist extension with a lateral offset constraining the index finger interface on a portion of a circular trajectory, compatible with the natural motion of the finger tip.

One unique feature of the sigma.7 device architecture is that rotational workspace is totally decoupled from translational workspace which means that full rotational dexterity is preserved in every translational position in space. In addition to this, the natural center of the user's hand corresponds to

TABLE I

SPECIFICATIONS OF THE SIGMA.7

	translation base	rotational wrist (axes 4,5,6)	grasping unit
workspace	$\emptyset 120mm$	$235, 140, 200deg$	$25mm$
resolution	$0.012mm$	$0.013deg$	$0.006mm$
output	$20N$	$0.4Nm$	$8N$

the center of rotation of the wrist extension, which avoids the static force/torque coupling arising in most pen-based haptic devices where there is an offset distance between user hand center and device wrist center of rotation. Hence, high forces can be displayed to the user's hand while preserving fine torque sensitivity. The haptic device is fully gravity compensated and it displays low perceived friction which helps keeping user fatigue low over longer periods of use.

The haptic device controller is hosted in a separate box which offers USB 2.0 connectivity to a control loop running on a PC. Measured encoder values are synchronously read out and locally time stamped, to ensure lowest jitter and optimal control loop design. High bandwidth motor drivers are updated with commanded torque values and a watch dog is included for safety. Closed-loop refresh rates of up to 8kHz can be achieved through asynchronous USB protocol on Windows, Linux or Mac OS X based systems. In the MiroSurge setup, QNX Neutrino real-time kernel 6.3 is used at 4kHz refresh rate. Four programmable input channels are used to interface the foot pedals of the operator console and a dead man switch disables forces.

B. Bi-manual console

With the telerobotic approach the ergonomics for the surgeon changes significantly from working beside the patient to sitting at a remote computerized workplace. Known health issues in manual laparoscopic surgery, like eye, neck, and back syndromes[11] could be avoided. Therefore, ergonomics played an important role in the design of the bi-manual console presented in this paper.

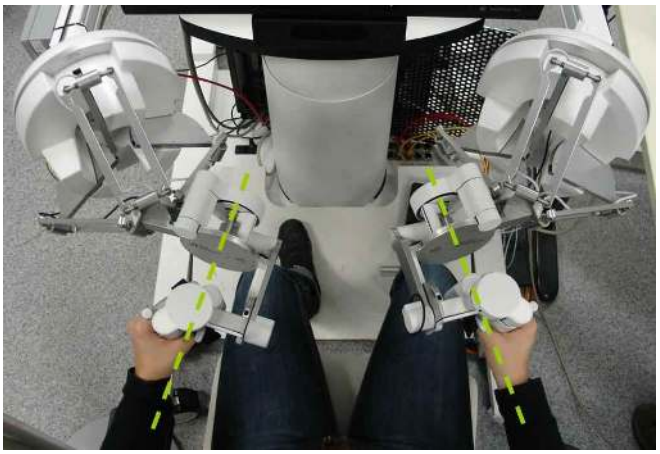

Fig. 5. Bi-manual configuration with axis 4 aligned with the forearm

The console integrates two sigma.7 devices, an auto-stereoscopic 3D monitor, computing power, and foot pedals for the clutch mode. With the use of auto-stereoscopic 3D displays no fixed position of the surgeon's head in relation to the console is required anymore, as it is with binocular displays. By this, a more flexible body posture of the surgeon is enabled. Furthermore, a more natural visual and aural communication with the other operating room personnel (e.g. scrub nurse) can be established. Searching for a single ideal configuration for all surgeons is not sensible, regarding e.g. the different body heights or already existing health issues of the surgeon.

The presented console therefore targets adaptability to the different needs of surgeons. Figure 6 shows two possible configurations of the bi-manual console. Due to the actuated lifting column, switching between these configurations takes only 4s (maximum travel time of the column). Additionally, the monitor position can be adapted. To oblige the preferences of the surgeons, various chairs or stools can be used, such that the surgeon can operate in different postures from leaned back to sitting upright or standing. For assistance of the arms the forearm rests of the chair or additional deployable arm rests can be utilized.

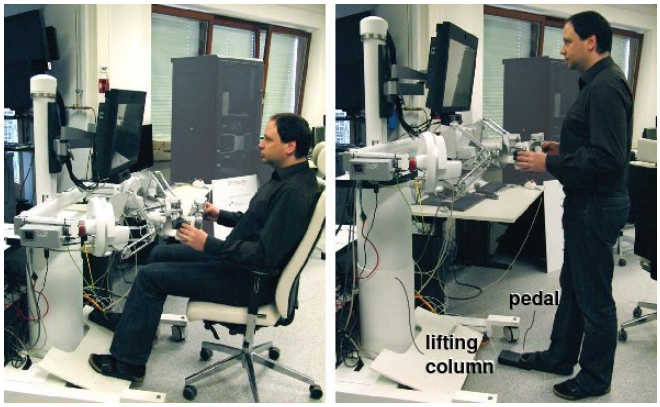

Fig. 6. Configuration of the bi-manual console for sitting (left) and standing (right)

III. Kinematics and dynamics

The kinematic and dynamic model of the device, as presented in this section, takes the HCP as the focus point (Fig. 4). Cartesian motion is described, as motion of the HCP-frame with respect to the Base-frame, which is coincident with the HCP in its nominal pose (center of workspace). Grasping is considered an independent functional DoF. The total inertia of the device is composed of the motor, link and handle inertia.

A. Jacobian

From a kinematics point of view, the sigma.7 device can be advantageously described by completely decoupling the translational workspace from the rotational one. The Jacobian $\mathbf{J}(\theta) = \frac{\delta \mathbf{x}}{\delta \theta}$ with Cartesian space $\mathbf{x} \in \Re^6$ and joint space $\theta \in \Re^6$, referring to axis 1 to 6, consists of two independent Jacobian matrices of dimension 3×3.

$$\mathbf{J}(\theta) = \begin{pmatrix} \mathbf{J}_t(\theta_t) & \mathbf{0} \\ \mathbf{0} & \mathbf{J}_r(\theta_r) \end{pmatrix} \quad (1)$$

The Jacobian for translations in the center of the workspace $\theta_{t,0} = (0.351, 0.351, 0.351)[rad]$ is:

$$\mathbf{J}_t(\theta_{t,0}) = \begin{pmatrix} 0.025704 & 0.068306 & -0.016898 \\ -0.025704 & 0.016898 & -0.068306 \\ -0.069570 & 0.034785 & 0.034785 \end{pmatrix} \quad (2)$$

The underlying parallel kinematics structure is highly decoupled with respect to its 3 joint parameters in the center of the workspace. This can be observed in the almost anti-diagonal form of the Jacobian matrix,

$$\mathbf{R}_z(-3pi/4)\mathbf{R}_y(pi/4)\mathbf{R}_z(pi/4) * \mathbf{J}_t(\theta_{t,0}) =$$

$$\begin{pmatrix} 0.0166 & 0.0070 & -0.0782 \\ 0.0166 & -0.0782 & 0.0070 \\ -0.0749 & -0.0011 & -0.0011 \end{pmatrix}$$

which results from a rotation of the Cartesian reference frame. The axis of the new reference frame, Rx*, Ry* and Ry* as shown in Fig. 3, are tending to be aligned with the parallel bar pairs. In addition, its variability is low in the constrained spherical sub-workspace of diameter $120mm$.

For the rotational part, the underlying XYZ Euler wrist structure is totally decoupled in its nominal orientation $\theta_{r,0} = (0,0,0)[rad]$, where its Jacobian matrix

$$\mathbf{J}_r(\theta_{r,0}) = \mathbf{I} \quad (3)$$

equals the identity matrix. The static decoupling of translations and rotations follows directly from the kinematic decoupling, since the Cartesian forces and torques are linked with the joint torques by the transposed Jacobian.

B. Link and motor inertia

In the dynamics equations, the translational base is not completely decoupled from the rotational wrist since the center of mass of the mobile parts of the wrist structure is not coincident with its center of rotation. This offset of less than $39mm$ distance introduces some dynamic coupling of low magnitude, which is barely noticeable to the operator under normal usage of the input device. The six dimensional link mass matrix takes into account all link masses and inertia, with exception of parallel bars inertia.

$$\mathbf{M}_l(\theta) = \begin{pmatrix} \mathbf{M}_{l,tt}(\theta) & \mathbf{M}_{l,tr}(\theta) \\ \mathbf{M}_{l,tr}(\theta)^T & \mathbf{M}_{l,rr}(\theta_r) \end{pmatrix} \quad (4)$$

For the usage as a haptic input device with relatively slow motion of the human hand during teleoperation of a remote surgical manipulator or simulation of a procedure in virtual reality, Coriolis and centrifugal terms are neglected throughout the dynamics modeling. In the center of the workspace $\theta_0 = [\theta_{t,0}; \theta_{r,0}]$, the 3×3 sub-matrices in $[10^{-3} kgm^2]$ are:

$$\mathbf{M}_{l,tt}(\theta_0) = \begin{pmatrix} 8.6989 & -1.2139 & -1.2139 \\ -1.2139 & 8.6989 & -1.2138 \\ -1.2139 & -1.2138 & 8.6989 \end{pmatrix}$$

$$\mathbf{M}_{l,rr}(\theta_{r,0}) = \begin{pmatrix} 1.4278 & -0.0240 & 0.0194 \\ -0.0240 & 0.5019 & 0.0000 \\ 0.0194 & 0.0000 & 0.2333 \end{pmatrix}$$

$$\mathbf{M}_{l,tr}(\theta_0) = \begin{pmatrix} 0.9161 & 0.3561 & -0.1242 \\ -0.4496 & -0.0370 & 0.08168 \\ -0.6282 & -0.1851 & -0.3302 \end{pmatrix}$$

Dynamic Coupling is very low inside the two diagonal sub-matrices $\mathbf{M}_{l,tt}(\theta_0)$ and $\mathbf{M}_{l,rr}(\theta_{r,0})$, the matrices are nearly diagonal due to inherent decoupling. The anti-diagonal submatrices $\mathbf{M}_{l,tr}(\theta)$ and its transpose are non-zero, which shows some dynamic coupling between the translational base and rotational wrist structure, as indicated above.

The motor rotor inertia expressed in joint space form the diagonal elements of matrix (in $[10^{-3}kgm^2]$)

$$\mathbf{B} = diag(1.011, 1.011, 1.011, 0.0178, 0.0145, 0.062) \quad (5)$$

which are roughly an order lower than the corresponding the diagonal elements of the link mass matrix $\mathbf{M}_l(\theta_0)$ in the center of the workspace.

In addition to the motor and link inertia the device dynamics are also influenced by the dynamics of the grasping unit, which has a mass of $m_h = 0.259[kg]$.

IV. Control with force/torque sensor

In this section a controller using the force-/torque sensor of the sigma.7 is presented. The idea is to feed back the measured wrench to reduce inertia and friction. The controller is implemented in joint space. The resulting torque controller can be interpreted as a scaling of the device admittance. Even though the sigma.7 already shows low inertia and friction without force control, the strong motors for all seven DoF and the rigidly designed mechanics have a certain influence. In minimally invasive robotic surgery the device usage goes beyond hard contact discrimination to perception of small stiffness variations of soft tissue. Especially for sensitive palpation tasks, e.g. for detecting and localizing a tumor, lower inertia and friction are beneficial to increase the transparency.

In literature, modifying the dynamics of haptic interfaces with force control is widely addressed. However, most controller designs and analysis only refer to a single DoF, e.g. [5] [3] [4]. It is also assumed that the force/torque sensor measures the external force of the human operator, i.e. the human touches the sensor directly. In this section a controller is introduced that feeds back the measured force as an internal state. It is theoretically shown that the controller reduces inertia over the whole workspace, as well as the friction, while the non-linear closed loop dynamics behave like a passive system. Two experiments are presented that show the closed loop behavior.

A. Model

For designing and analyzing the controller, the device dynamics is split up into two parts connected by the sensor: 1) the translational base and rotational wrist with motors and joints of axis 1 to 6, as well as the links; 2) the grasping unit (or handle). The controller presented here, refers to the first part with axes 1 to 6 that are required for motion in space. The grasping is considered to be a separate functional DoF and the grasping unit is consequently treated as a passive handle attached to the force/torque sensor. In Fig. 7 a model of the device is shown with all states/input/output variables projected into the 6 DoF joint space. The motor torque τ_m is actuating the motor inertia $\mathbf{B}$ that is assumed to be rigidly connected with the link inertia $\mathbf{M}_l$. Additionally, friction τ_{fric} and the sensor torque τ_s are affecting the motor and link motion.

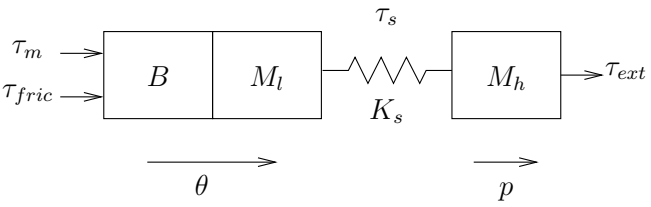

Fig. 7. Physical model of the sigma with the force/torque sensor as a spring; motor and link inertia are left; handle inertia is on the right side

The motor/link dynamics

$$(\mathbf{B} + \mathbf{M}_l(\theta))\ddot{\theta} + \mathbf{C}_l(\theta, \dot{\theta})\dot{\theta} + \mathbf{g}_l(\theta) + \tau_s + \tau_{fric} = \tau_m \quad (6)$$

is completed with the centripetal-/coriolis forces $\mathbf{C}_l(\theta, \dot{\theta})\dot{\theta}$ and gravity $\mathbf{g}_l(\theta)$, where $\theta \in \Re^6$ represents the motor sided joint angles. The handle sided angles in joint space are given with $\mathbf{p}$ in the dynamics of the handle:

$$\mathbf{M}_h(\mathbf{p})\ddot{\mathbf{p}} + \mathbf{C}_h(\mathbf{p}, \dot{\mathbf{p}})\dot{\mathbf{p}} + \mathbf{g}_h(\mathbf{p}) = \tau_s + \tau_{ext} \quad (7)$$

The external force τ_{ext} is an unmeasured input, whereas the sensor torque τ_s is modeled as an internal state. It connects motor and handle positions

$$\tau_s = \mathbf{K}_s(\theta - \mathbf{p}) \quad (8)$$

with the sensor stiffness $\mathbf{K}_s$.

Furthermore, the model has the following properties:
P1: the link mass matrix is symmetric and positive definite: $\mathbf{M}_l(\theta) = \mathbf{M}_l(\theta)^T > 0; \forall \theta \in \Re^6$
P2: the matrix $\dot{\mathbf{M}}_l(\theta) - 2\mathbf{C}_l(\theta, \dot{\theta})$ is screw-symmetric : $\mathbf{y}(\dot{\mathbf{M}}_l(\theta) - 2\mathbf{C}_l(\theta, \dot{\theta})) = 0; \forall \mathbf{y}, \theta, \dot{\theta} \in \Re^6$
P3: gravity of the handle $\mathbf{g}_h(\mathbf{p})$ is given as a differential of a globally bounded potential function $V_{g_h}(\mathbf{p})$ with $\mathbf{g}_h(\mathbf{p}) = (\delta V_{g_h}(\mathbf{p})/\delta \mathbf{p})^T$
P4: friction is given as a passive function of the motor sided joint velocity: $(\dot{\theta} \rightarrow \tau_{fric})$

B. Controller

A state feedback controller can be selected,

$$\tau_m = r \cdot \mathbf{u} + (1-r)\tau_s + \mathbf{g}_l(\theta) \tag{9}$$

where r is a positive gain. The vector $\mathbf{u}$ represents a new torque input. The control uses the measured joint angles and the measured wrench of the force/torque sensor transformed into joint space with the Jacobian. Inserting (9) into (6) leads to the closed loop dynamics of the motor/link system. Inertia, friction and centripetal-/coriolis forces are reduced proportional to r^{-1}.

$$r^{-1}(\mathbf{B} + \mathbf{M}_l(\theta))\ddot{\theta} + r^{-1}\mathbf{C}_l(\theta,\dot{\theta})\dot{\theta} + \tau_s + r^{-1}\tau_{fric} = \mathbf{u} \tag{10}$$

Gravity of the links can be fully compensated. Adding gravity compensation of the handle

$$\mathbf{u} = -\mathbf{u}_{app} + \mathbf{g}_h(\bar{\theta}) \tag{11}$$

gives the application input $\mathbf{u}_{app}$. Gravity compensation is based on a motor sided estimation of the handle sided angles $\bar{\theta}$, which is statically equivalent to $\mathbf{p}$ and must be iteratively approximated in implementation [10]. However, in the given case of a quite stiff sensor[1], one can simply use $\bar{\theta} \approx \theta$, which is equivalent to the initial value of the approximation with zero iterations . The controller design covers the general case of $\mathbf{K}_s$.

C. Passivity

Passivity is a desirable property of a haptic device, due to: 1) Robustness in contact; 2) Modularity in connection with applications. The later is of particular interest here. The controller design is motivated by requirements from robotic surgery, but should not be restricted to a particular application. In Fig. 8 the system is shown as a degenerative connection of passive subsystems [14]. The human operator

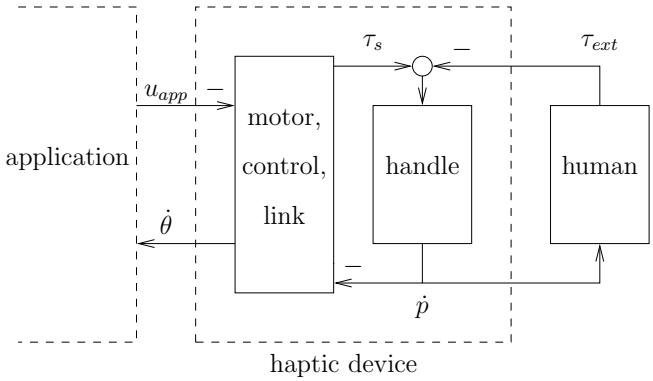

Fig. 8. System with haptic device, human operator and application as interconnection of passive subsystems

is typically assumed to be passive. The handle dynamics given by (7) is passive too, since there is no motor as an active component. The application needs to be passive with an impedance port of ingoing velocities and outgoing forces(torques). That is the only restriction on the application. It can, e.g. be a robotic telesurgery system, a fine assembly simulation or simply a virtual wall. What remains to be shown, is that the block with motors, control and links is passive. In general, it can potentially be active due to the actuators.

A system ($\mathbf{u} \rightarrow \mathbf{y}$) is passive, if there exists a continuous storage function S [12], which is bounded from below and for which the derivative satisfies the inequality $\dot{S} \leq \mathbf{y}^T\mathbf{u}$.

Inserting (11) into (10) gives the dynamics of the motor/control/link subsystem.

$$\frac{1}{r}(\mathbf{B} + \mathbf{M}_l(\theta))\ddot{\theta} + \frac{1}{r}\mathbf{C}_l(\theta,\dot{\theta})\dot{\theta} + \mathbf{u}_{app} + \tau_s + \frac{1}{r}\tau_{fric} = \mathbf{g}_h(\bar{\theta}) \tag{12}$$

The storage function as a mapping of ($\dot{\mathbf{p}} \rightarrow \tau_s$) is given by

$$S = \frac{1}{2r}\dot{\theta}^T(\mathbf{B} + \mathbf{M}_l(\theta))\dot{\theta} + \frac{1}{2}(\theta - \mathbf{p})^T\mathbf{K}_s(\theta - \mathbf{p}) - V_{g_h}(\bar{\theta}) \tag{13}$$

with the kinetic energy of the scaled inertia and the potential energy of the spring (sensor) and the gravity. The energy of the inertia and the spring are greater or equal zero and gravitational energy is lower bounded. It follows directly that S is lower bounded. Furthermore, with gravity compensation based on $\mathbf{g}_h(\bar{\theta})$ the device is in a static equilibrium in any pose. The derivative

$$\dot{S} = -r^{-1}\dot{\theta}^T\tau_{fric} - \dot{\theta}^T\mathbf{u}_{app} - \dot{\mathbf{p}}^T\tau_s \tag{14}$$

describes the power balance, with friction, which is passive by definition, and the two ports of the block. It follows that the motor/control/link subsystem is passive, if the ports, i.e. the connected subsystems are passive.

D. Experiments

The above described controller structure with the force/torque sensor was tested in experiments with one sigma.7. The admittance scaling factor was chosen to be $r^{-1} = 0.5$, i.e. the effective inertia of the motor $\mathbf{B}$ and the links $\mathbf{M}_l$, as well as friction τ_{fric} are half the ones of the open loop device. Two experiments were done with translational motion in the z-axis in upward and downward direction. The first experiment was also done in 6 DoF. All tests were done with admittance scaling ($r^{-1} = 0.5$) and without admittance scaling ($r = 1$).

1) Human motion: In the first experiment a human operator holds the device in his hand and moves it up and down in a sinusoidal motion for 5 seconds, as shown in Fig. 9. The controller is switched off first (left,top). Then it is switched on and the human tries to perform a similar motion (right,top). The corresponding forces, that are measured with the sensor are shown in the lower graphs. It can be seen that the force magnitude is reduced with the controller, whereas frequency and magnitude of the resulting velocity is almost the same. The average absolute velocity without the controller is $v_1 = 0.1007\frac{m}{s}$ (dashed line, top, left), with the controller it is $v_2 = 0.1062\frac{m}{s}$ (dashed line, top, right). The average absolute forces the user needs to generate this motion are $f_1 = 1.121N$ (dashed line, bottom, left) and

[1]translational stiffness $\geq 10^6\frac{N}{m}$; www.ati-ia.com; February 2011

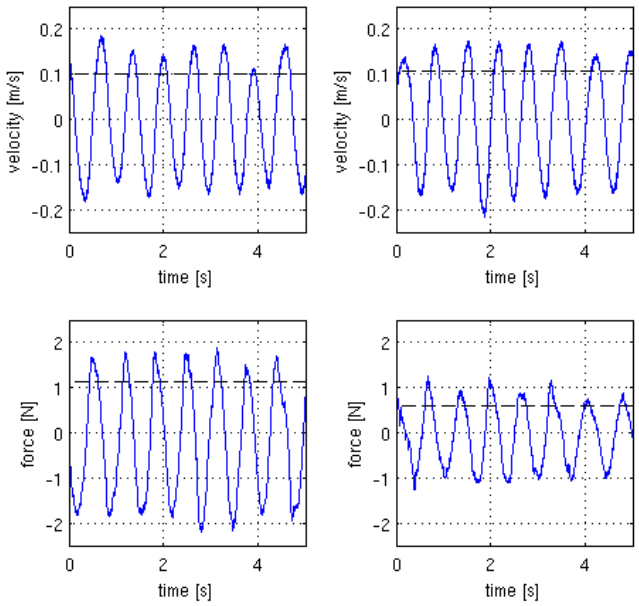

Fig. 9. Sinusoidal motion of human operator in z-axis; Left: velocity and measured force without admittance scaling; Right: velocity and measured force with admittance scaling

$f_2 = 0.590N$ (dashed line, bottom, right). A experimental admittance scaling factor can be determined by dividing the open loop admittance by the closed loop admittance:

$$\frac{\frac{v_1}{f_1}}{\frac{v_2}{f_2}} = 0.498 \tag{15}$$

The result is very close to the expected value of 0.5. The experiment was repeated with motion in 6 DoF for 5 seconds with and without admittance scaling. Experimental scaling factors were evaluated for the six joints, as described above. The resulting scaling factors were between 0.45 and 0.55 for the three joints of the translational base and between 0.35 and 0.65 for the three joints of the wrist. The derivation is due to the limited human ability of performing repeated, periodic motion in 6 DoF and the non-linear dynamics of the haptic device, in particular friction.

2) External mass: In the second experiment a small external mass was attached to the handle of the sigma.7. The load of the mass is about $0.6N$. It was chosen to demonstrate how the admittance scaling reduces friction. In the experiments an impedance (PD-) controller initially holds the mass against gravity around the zero position in the middle of the workspace. The impedance controller is switched off and the mass moves the handle downwards against a virtual wall. In Fig. 10 the results are shown without and with control, in left and right graphs, respectively. Without torque control the handle starts to move and gets stopped by the friction (left, top). The measured force simply shows the load of $-0.6N$ in z-direction. When repeating the experiment with the controller the device falls onto the virtual wall at $-0.05m$ on the z-axis (dashed line, top, right) and bounces back. It eventually settles in a stable contact. The force signal (bottom, right) shows peaks, when hitting the virtual wall. In hard contacts not only the external mass, but also the mass of the handle, which is statically compensated, significantly contributes to the inertia causing the force peaks.

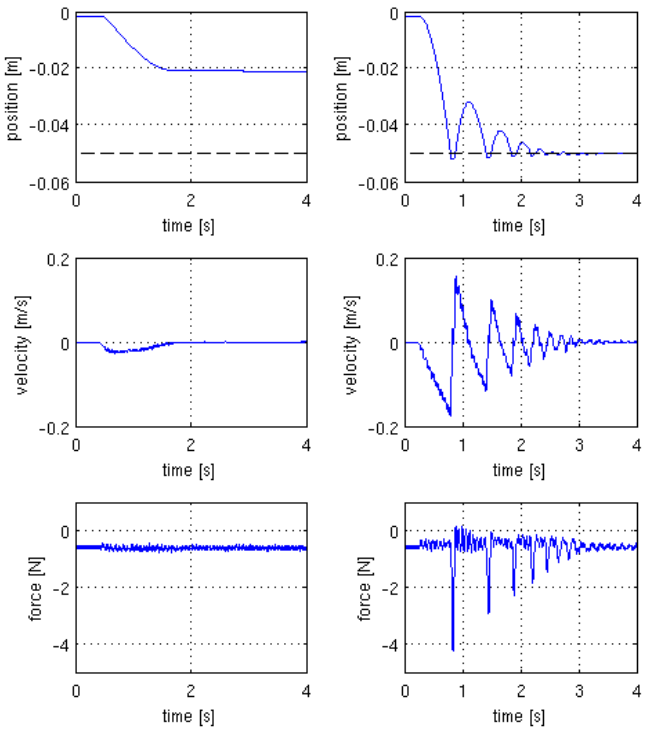

Fig. 10. External load falls against a virtual wall in z-axis; Left: position, velocity and measured force without dynamic scaling; Right: position, velocity and measured force with dynamic scaling

V. Conclusion

In this paper the new bi-manual surgical console of MiroSurge was presented. The custom designed sigma.7 haptic devices combine a rotational workspace sufficient for suturing, a rigid mechanical structure and strong motors. The device is capable of 6 DoF force/torque feed back, with continuous 20N and 0.4Nm, respectively. An actuated grasping unit offers an additional functional DoF. The inertia and friction of the device is low for fatigue-proof operation and can be further reduced for fine palpation of tissue by means of control. The controller uses an integrated force/torque sensor to implement an admittance scaling of the haptic device. Validating experiments were presented and passivity was theoretically shown for the whole non-linear workspace. The device dynamics is inherently decoupled with the inertia matrix being nearly diagonal in the center of the workspace. The translational base and the rotational wrist are kinematically and statically decoupled, which can be observed in the Jacobian. Dedicated left and right handed devices were integrated into an ergonomic surgical console. The console features an adjustable auto-stereoscopic 3D-Display and a lifting column for seated and standed operation.

The surgical console is fully integrated into the DLR MiroSurge system for minimally invasive robotic surgery. It

was used in suturing and palpation tasks. The design of the device and the console will be evaluated with surgeons and experiments with the MiroSurge system will be done.

VI. Acknowledgment

The research leading to these results has received funding from the European Union Seventh Framework Programme (FP7/2007- 2013) under grant agreement n248960.

References

[1] *PHANToM haptic interface: a device for probing virtual objects*, volume 55-1 of *Proceedings of the 1994 International Mechanical Engineering Congress and Exposition*, Massachusetts Inst of Technology, Cambridge, United States. ASME.

[2] Hayward Gregorio Astley, V. Hayward, P. Gregorio, O. Astley, S. Greenish, M. Doyon, L. Lessard, J. Mcdougall, I. Sinclair, S. Boelen, X. Chen, J. p. Demers, J. Poulin, I. Benguigui, N. Almey, B. Makuc, and X. Zhang. Freedom-7: A high fidelity seven axis haptic device with application to surgical training. In *Lecture Notes in Control and Information Science 232*, pages 445–456. Springer Verlag, 1997.

[3] Nicholas L. Bernstein, Dale A. Lawrence, and Lucy Y. Pao. Friction modeling and compensation for haptic interfaces. In *Proceedings of the First Joint Eurohaptics Conference and Symposium on Haptic Interfaces for Virtual Environment and Teleoperator Systems*, WHC '05, pages 290–295, Washington, DC, USA, 2005. IEEE Computer Society.

[4] Göran A. Christiansson. Wave variables and the 4 channel architecture for haptic teleoperation. In *Proceedings of the 6th international conference on Haptics: Perception, Devices and Scenarios*, EuroHaptics '08, pages 169–174, Berlin, Heidelberg, 2008. Springer-Verlag.

[5] Jorge Juan Gil and Emilio Sanchez. Control algorithms for haptic interaction and modifying the dynamical behaviour of the interface. In *Proceedings of Enactive, Genova, Italy*, 2005.

[6] S. Grange, F. Conti, P. Rouiller, P. Helmer, and C. Baur. The Delta Haptic Device. In *Mecatronics 2001*, 2001.

[7] U. Hagn, R. Konietschke, A. Tobergte, M. Nickl, S. Jörg, B. Kuebler, G. Passig, M. Gröger, F. Fröhlich, U. Seibold, L. Le-Tien, A. Albu-Schäffer, A. Nothelfer, F. Hacker, M. Grebenstein, and G. Hirzinger. DLR MiroSurge - a versatile system for research in endoscopic telesurgery. *International Journal of Computer Assisted Radiology and Surgery*, 2009.

[8] U. Hagn, T. Ortmaier, R. Konietschke, B. Kuebler, U. Seibold, A. Tobergte, M. Nickl, S. Jörg, and G. Hirzinger. Telemanipulator for remote minimally invasive surgery. *IEEE Robotics & Automation Magazine*, 15(4):28–38, December 2008. DOI: 10.1109/MRA.2008.929925.

[9] T. Hulin, M. Sagardia, J. Artigas, S. Schätzle, P. Kremer, and C. Preusche. Human-scale bimanual haptic interface. In *Enactive08*, pages 28–33, Pisa, Italy, Nov. 2008.

[10] Ch. Ott, A. Albu-Schäffer, A. Kugi, S. Stramigioli, and G. Hirzinger. A passivity based Cartesian impedance controller – part I: Torque feedback and gravity compensation. In *Proceedings of the IEEE International Conference on Robotics and Automation (ICRA)*, New Orleans, USA, 2004.

[11] Adrian Park, Gyusung Lee anf F. Jacob Seagull, Nora Meenaghan, and David Dexter. "patients benefit while surgeons suffer: An impending epidemic". *J Am Coll Surg*, 210(3):306–313, 2010.

[12] A. J. Van der Schaft. *L2-Gain and Passivity Techniques in Nonlinear Control*. Springer-Verlag New York, Inc., Secaucus, NJ, USA, 1st edition, 1996.

[13] U. Seibold, B. Kuebler, and G. Hirzinger. Prototypic force feedbackinstrument for minimally invasive robotic surgery. In V. Bozovic, editor, *Medical Robotics*, pages 377–400. I-Tech Education and Publishing, Vienna, Austria, 2008.

[14] Jean-Jacques Slotine and Weiping Li. *Applied Nonlinear Control*. Prentice Hall, October 1990.

[15] Sophie Thielmann, Ulrich Seibold, Robert Haslinger, Georg Passig, Thomas Bahls, Stefan Jörg, Mathias Nickl, Alexander Nothhelfer, Ulrich Hagn, and Gerd Hirzinger. Mica - a new generation of versatile instruments in robotic surgery. In *Proceedings of IROS'10, the IEEE International Conference on Intelligent Robots and Systems*, 2010.

[16] A. Tobergte, R. Konietschke, and G. Hirzinger. Planning and control of a teleoperation system for research in minimally invasive robotic surgery. In *Proceedings of the IEEE International Conference on Robotics and Automation (ICRA)*, pages 4225–4232, 2009.

[17] Andreas Tobergte, Georg Passig, Bernhard Kübler, Ulrich Seibold, Ulrich Hagn, Florian Fröhlich, Rainer Konietschke, Stefan Jörg, Mathias Nickl, Sophie Thielmann, Robert Haslinger, Martin Gröger, Alexander Nothhelfer, Luc Le-Tien, Robin Gruber, Alin Albu-Schäffer, and Gerd Hirzinger. Mirosurge - advanced user interaction modalities in minimally invasive robotic surgery. *PRESENCE - Teleoperators and Virtual Environments*, Vol. 19(5):400–414, 2010.

[18] Hagn U., Nickl M., Jörg S., Passig G., Bahls T., Nothhelfer A., Hacker F., Le-Tien L., Albu-Schäffer A., Konietschke R., Grebenstein M., Warpup R., Haslinger R., Frommberger M., and Hirzinger G. The DLR MIRO: A versatile lightweight robot for surgical applications. In *Industrial Robot: An International Journal2008*.